Monthly Notices
of the
ROYAL ASTRONOMICAL SOCIETY

Mon. Not. R. Astron. Soc. **421,** 25–35 (2012) doi:10.1111/j.1365-2966.2011.19811.x

The dark GRB 080207 in an extremely red host and the implications for gamma-ray bursts in highly obscured environments

K. M. Svensson,[1] A. J. Levan,[1⋆] N. R. Tanvir,[2] D. A. Perley,[3] M. J. Michalowski,[4] K. L. Page,[2] J. S. Bloom,[3] S. B. Cenko,[3] J. Hjorth,[5] P. Jakobsson,[6] D. Watson[5] and P. J. Wheatley[1]

[1]*Department of Physics, University of Warwick, Coventry CV4 7AL*
[2]*Department of Physics and Astronomy, University of Leicester, Leicester LE1 7RH*
[3]*Department of Astronomy, University of California, Berkeley, CA 94720-3411, USA*
[4]*Scottish Universities Physics Alliance, Institute for Astronomy, University of Edinburgh, Royal Observatory, Edinburgh EH9 3HJ*
[5]*Dark Cosmology Centre, Niels Bohr Institute, University of Copenhagen, Juliane Maries Vej 30, DK-2100 Copenhagen, Denmark*
[6]*Centre for Astrophysics and Cosmology, Science Institute, University of Iceland, Dunhagi 5, IS-107 Reykjavik, Iceland*

Accepted 2011 September 12. Received 2011 September 5; in original form 2010 October 21

ABSTRACT

We present comprehensive X-ray, optical, near- and mid-infrared and submm observations of GRB 080207 and its host galaxy. The afterglow was undetected in the optical and near-infrared (nIR) implying an X-ray-to-optical spectral slope less than 0.3, identifying GRB 080207 as a dark burst. *Swift* X-ray observations show extreme absorption in the host, which is confirmed by the unusually large optical extinction found by modelling the X-ray to nIR afterglow spectral energy distribution. Our *Chandra* observations obtained 8 d post-burst allow us to place the afterglow on the sky to subarcsec accuracy, enabling us to pinpoint an extremely red galaxy (ERO), with $R - K > 5.4$ ($g - K \sim 7.5$, VEGAmag) at the afterglow location. Follow-up host observations with the *Hubble Space Telescope*, *Spitzer Space Telescope*, Gemini, Keck and the James Clerk Maxwell Telescope provide a photometric redshift solution of $z \approx 1.74^{+0.05}_{-0.06}$ (1σ, $1.56 < z < 2.08$ at 2σ) for the ERO host, and suggest that it is a massive and morphologically disturbed ultraluminous infrared galaxy system, with $L_{\rm FIR} \sim 2.4 \times 10^{12}\,{\rm L}_{\odot}$. These results add to the growing evidence that gamma-ray bursts (GRBs) originating in very red hosts always show some evidence of dust extinction in their afterglows (though the converse is not true – some extinguished afterglows are found in blue hosts). This indicates that a poorly constrained fraction of GRBs occurs in very dusty environments. By comparing the inferred stellar masses, and estimates of the gas phase metallicity in both GRB hosts and submm galaxies we suggest that many GRB hosts, even at $z > 2$, are at lower metallicity than the submm galaxy population, offering a likely explanation for the dearth of submm-detected GRB hosts. However, we also show that the dark GRB hosts are systematically more massive than those hosting optically bright events, perhaps implying that previous host samples are severely biased by the exclusion of dark events.

Key words: gamma-ray burst: general.

1 INTRODUCTION

A fraction of gamma-ray burst (GRB) afterglows are undetected or have suppressed flux in the optical and even in the near-infrared (nIR; e.g. Groot et al. 1998). These bursts may include high-redshift events or where there is significant absorption in the host galaxy. Alternatively, observational selection effects may result in a non-detection due to unfavourable location, poor weather etc. for ground-based observatories. These observational selection effects can largely be avoided by selecting bursts based on some quantitative criteria, in particular by comparing the optical limits on the afterglow emission to the expected values based on the observed X-ray flux and spectral slope. By this criterion Jakobsson et al. (2004) (see also Rol et al. 2005) define dark bursts as those with an X-ray-to-optical spectral slope, $\beta_{\rm OX} < 0.5$, where $F_\nu \propto \nu^{-\beta}$

⋆E-mail: a.j.levan@warwick.ac.uk

and

$$\beta_{\rm OX} = \frac{\log_{10}(F_{\nu,\rm X}/F_{\nu,\rm Opt})}{\log_{10}(\nu_{\rm X}/\nu_{\rm Opt})}. \quad (1)$$

In the range $0.5 < \beta_{\rm OX} < 1.25$ which is suggested by the standard fireball model, the distribution of $\beta_{\rm OX}$ is approximately flat (e.g. fig. 1 in Jakobsson et al. 2004), with a tail of $\beta_{\rm OX} < 0.5$ outliers. van der Horst et al. (2009) proposed a more sophisticated approach and define dark bursts by $\beta_{\rm OX} < \beta_{\rm X} - 0.5$. Selecting bursts which are dark by these requirements, ensures the sample studied appears genuinely physically distinct from the optically bright GRBs, in contrast to simple requirement of an optical non-detection, which is often not constraining in terms of physical models of the afterglow (Rol et al. 2005). Understanding these dark bursts, and the physical causes of darkness is important, not only for characterizing the diversity of GRBs themselves, but also for establishing their utility as cosmological probes, and in particular as tracers of the global star formation rate (SFR).

Since long GRBs are known to be associated with massive stars (e.g. Hjorth et al. 2003; Stanek et al. 2003), we can contemplate an ideal scenario in which there was direct proportionality between GRB rate and SFR, allowing the GRB rate to be an immediate measure of the global SFR across cosmic history. Two particular advantages of GRBs in this role come from their brightness, allowing them to be seen at the most extreme redshifts (Salvaterra et al. 2009; Tanvir et al. 2009) and their high energy emission, enabling them to be seen through high dust columns. Coupled with this, they select galaxies across the luminosity function (rather than just at the bright end). Hence, GRBs have the potential to infer the SFR, largely free from the order of magnitude corrections that other techniques must apply. For example, estimates based on Lyman break galaxies must make corrections to account for missing galaxies at the faint end of the luminosity function (e.g. Bouwens et al. 2006; Bunker et al. 2010), and dust obscuration (e.g. Bouwens et al. 2009; Overzier et al. 2011). In contrast, submm searches find the most extreme, dusty examples, but (at least at present) cannot study fainter galaxies, and hence also require large-scale corrections to obtain a total SFR (Hughes et al. 1998; Blain et al. 1999). In practice however, the promise of GRBs remains to be fulfilled. This is largely due to a combination of incompleteness in the available samples (e.g. Jakobsson et al. 2006; Fynbo et al. 2009) for example because of the difficulty in locating dust obscured GRBs, and because of poorly known environmental effects (such as metallicity; e.g. Wolf & Podsiadlowski 2007; Modjaz et al. 2008) on the GRB progenitors which impact any direct proportionality between GRB rate and SFR. An understanding of dark bursts offers a route through both of these problems; by increasing the completeness of GRB samples, the ability to obtain an accurate redshift distribution for the whole of the GRB population currently detected by *Swift* is gained. In tandem, studies of the environments of dark bursts, in comparison with those of bright examples can be extremely valuable in elucidating the impact of environment on GRB production.

It is therefore reasonable to ask how studies of dark bursts can be achieved. GRBs are located in the gamma-rays and subsequently pinpointed by their X-ray afterglows. Although X-ray afterglows in the *Swift* era are ubiquitous, they frequently do not allow detailed study of the burst due to the inability to obtain either absorption spectroscopy of the afterglow, or the unambiguous detection of the host galaxy. Although *Swift* X-ray positioning has been greatly improved by more refined algorithms that determine the satellites pointing using the Ultraviolet and Optical Telescope (UVOT), the median X-Ray Telescope (XRT) error circle is still ∼1.5 arcsec, with 90 per cent of bursts being positioned to less than 2 arcsec (Evans et al. 2009) – suggesting that the bulk of GRB host galaxies still cannot be unambiguously determined using only X-rays; purely by chance (e.g. considering the galaxy number counts by Hogg et al. 1997), XRT error circles have ∼15 per cent probability of *randomly* containing a galaxy with $R < 25$ – roughly the median magnitude of GRB hosts (Hogg & Fruchter 1999), and may contain more than one galaxy comparable to the faintest known GRB hosts – $R < 29$ (Fruchter et al. 2006). Hence, even the now well-refined X-ray positions from the *Swift* XRT (Evans et al. 2007) cannot unambiguously locate a host. Although absorption in the X-ray afterglows can provide a clue to the GRB environment via the measurement of hydrogen column ($N_{\rm H}$), this is one of few constraints that can be obtained from the X-ray afterglow alone. Indeed, in the absence of a redshift, even the rest-frame X-ray column cannot be accurately constrained. Although the definition of dark bursts does not require an optical afterglow non-detection (and indeed in many cases the afterglow has been detected), selecting an unbiased sample of dark burst hosting galaxies calls for accurate identification of the host even in cases where the optical afterglow remains undetected. A possible solution to the problem of identifying the hosts is to obtain subarcsec astrometric positions, reducing the chance alignment by a factor of ∼10, for dark GRBs via their X-ray afterglows. Currently, this is only enabled by the *Chandra* X-ray Observatory, and this is the approach employed here.

A consequence of the relative dearth of dark bursts (per the $\beta_{\rm OX} < 0.5$ definition rather than simply optical non-detection, also throughout this work) in the pre-*Swift* era and relatively weak constraints which can be obtained from X-ray afterglows alone means that the origins and hosts of dark GRBs remain relatively poorly understood, despite the relatively large number uncovered by *Swift*. It is therefore not entirely clear how the environments (both local and galactic) of dark GRBs differ from those of the optically bright population. The fraction of dark bursts appears to be ∼0.5 (Melandri et al. 2008; Cenko et al. 2009; Fynbo et al. 2009) with the majority of these being consistent with low- to medium-redshift events suffering from dust extinction in the host (Perley et al. 2009), while perhaps ∼20 per cent originate from $z > 5$ (Greiner et al. 2011). This could significantly bias samples based on optical detections of the afterglow. Studying the host population of dark GRBs is therefore a priority in order to understand how they differ from normal bursts and what impact the difference will have on statistical host samples – either by inclusion of dark burst hosts, or by their exclusion. Although the number of dark GRBs with securely identified hosts is still relatively small it is noteworthy that several of other heavily extinguished bursts hitherto have been associated with galactic environments that are *atypical* of the overall host population: The hosts of GRB 020127 and GRB 030115 are massive extremely red objects (EROs; e.g. Levan et al. 2006a; Berger et al. 2007), although the $\beta_{\rm OX}$ values are poorly or unconstrained due to lacking follow-up observations (Fox & Frail 2002; Smith et al. 2005). GRB 051022 has a massive host (Svensson et al. 2010) with large average extinction (e.g. Castro-Tirado et al. 2007; Rol et al. 2007) and GRB 080325 also has a massive host with evidence of significant extinction (Hashimoto et al. 2010). Although this is not an exhaustive list of all dark bursts, in these cases the evidence seems to suggest either unusually red hosts, unusually massive hosts or hosts with very high extinction. It is also interesting to note that, in the sample of 34 GRBs in Svensson et al. (2010) where stellar masses are estimated from spectral energy distribution (SED) fitting, the hosts of all dark bursts are found to be above the median mass of the sample.

Here we present observations of GRB 080207 and its host, utilizing multiwavelength observations stretching from the X-ray to the submm to identify a host galaxy, and study its properties in comparison to other dark, and bright, GRB hosts.

2 OBSERVATIONS

GRB 080207 was discovered by *Swift* at 21:30:21 UT on 2008 February 7. A prompt slew enabled the location of an X-ray afterglow, however, no optical afterglow was found in UVOT observations. The burst was long duration with $t_{90} > 300$ s [at which point the source moved out of the Burst Alert Telescope (BAT) field of view; Stamatikos et al. 2008].

2.1 Afterglow

2.1.1 X-ray

Observations with the *Swift* XRT began 124 s after the burst, and continued for 30 h. For spectral analysis the XRT observations were first processed through XRTPIPELINE to create cleaned event lists in both window timing (WT) and photon counting (PC) mode. We separately fitted spectra to the WT and PC mode data using XSPEC. The WT data are best fitted by an absorbed power-law model with spectral slope $\beta = 0.34 \pm 0.1$ ($F_\nu \propto \nu^{-\beta}$), and $N_{\rm H} = (96 \pm 11) \times 10^{20}$ cm^{-2} (assuming zero redshift for the absorption), significantly in excess of the galactic value of 1.94×10^{20} cm^{-2}. The PC mode observations yielded a similar excess column density, $N_{\rm H} = (75 \pm 16) \times 10^{20}$ cm^{-2}, but a much softer spectral slope of $\beta = 1.4 \pm 0.1$. It is also worth noting that a consistently high $N_{\rm H}$ for the zero redshift case was also found by Racusin (2008).

The WT mode observations took place during the period 130 to 194 s post-burst. Throughout this time the BAT was also detecting higher energy emission, and the harder spectral index measured in the WT data is most likely a consequence of the prompt emission in the X-ray band. We therefore adopt the spectral slope of the afterglow as $\beta = 1.4 \pm 0.1$, as measured in the PC mode observations.

We took the X-ray light curve from the *Swift* repository (Evans et al. 2007, 2009), to which we added the *Chandra* observation at $t \sim 7 \times 10^5$ s. The light curve is roughly flat during the WT mode observations. The period between the end of WT and the beginning of PC mode observations is broadly consistent with a single power-law decay ($F(t) \propto t^{-\alpha}$) of index $\alpha \sim 1.0$. There is no sign of, or requirement for steep initial decays, or a later time plateau as seen in many X-ray afterglows (Nousek et al. 2006). The PC mode late time (between 1000 and 10^6 s) (Fig. 1) is fitted with a single power law with a decay index $\alpha = 1.7 \pm 0.1$ and χ^2/dof = 65.36/65 $\sim$ 1.005.

Chandra observed the afterglow of GRB 080207 on 2008 February 16. The afterglow was placed on the AXAF CCD Imaging Spectrometer (ACIS) S-3 (back illuminated) chip and very faint (VF) mode employed to enable better rejection of background events. The standard cleaned event files were utilized, but filtered to the energy range of 0.5–7 keV (largely to reduce background events and better isolate the afterglow). The afterglow was detected at a position of RA = $13^{\rm h}50^{\rm m}02\overset{\rm s}{.}98$, Dec. = $07^\circ30'07\overset{''}{.}4$ (J2000) with a 0.5 arcsec error circle. The background subtracted count rate of the afterglow in this band was found to be 5.3×10^{-4} s^{-1}. There are insufficient counts in the image to obtain a spectrum directly, however, by assuming the same spectral index as measured in the *Swift* PC mode data this implies a flux of 3.8×10^{-15} erg s^{-1} cm^{-2} in the 0.3–10 keV band equivalent to *Swift*/XRT, and is consistent to $\sim 1\sigma$ with the extrapolation of the earlier X-ray light curve – indicating that any jet break has jet to occur 8 d post-burst. Alternatively the jet break could have occurred earlier than the onset of the PC mode observations ($\sim$5000 s), although this is unusual.

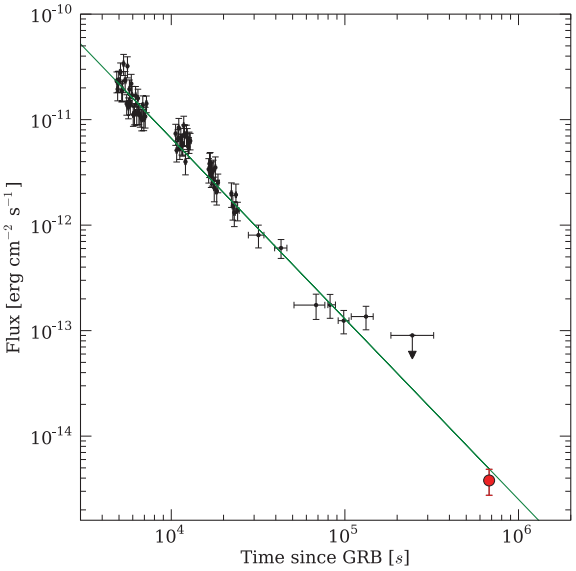

Figure 1. The X-ray light curve of GRB 080207 from *Swift*/XRT PC mode (small black points) and *Chandra* (large filled circle). The *Chandra* flux is rescaled from its observed ACIS bandwidth to equivalent of the *Swift*/XRT in this figure. The solid green line shows a single power-law fit with a decay slope $\alpha = 1.7$.

2.1.2 Optical

Deep optical observations of GRB 080207 were pursued by several groups roughly 12 h after the GRB and include observations by 2 to 8 m class telescopes in both the optical and nIR. None of these observations yielded any afterglow candidates to deep limits. Kuepcue Yoldas et al. (2008) report deep optical limits from the Gamma-Ray Burst Optical/Near-Infrared Detector (GRON)D: $g' > 23.9, r' > 23.8, i' > 23.5$ and $z' > 22.8$, nIR limits from the Very Large Telescope (VLT) are reported by Fugazza et al. (2008) as $J > 23.5, H > 22.8$ and $K > 21.5$.

These limits are amongst the deepest obtained for emission from any GRB at moderate times after the burst ($\sim$12 h), and were obtained across the optical and nIR waveband by the dual use of multiple 8-m telescopes. The deep limits in both the optical and the IR rule out colours similar to that of high-z GRBs like 050814 (Jakobsson et al. 2006), 050904 (Haislip et al. 2006; Kawai et al. 2006), 080913 (Greiner et al. 2009; Patel et al. 2010; Pérez-Ramírez et al. 2010), 090423 (Salvaterra et al. 2009; Tanvir et al. 2009) and 090429B (Cucchiara et al. 2011), and also very red colours due to extinction as have been observed in a handful of bursts (e.g. Levan et al. 2006a; Rol et al. 2007; Jaunsen et al. 2008; Tanvir et al. 2008).

2.2 Astrometry

To locate the X-ray afterglow precisely on the deep host galaxy images, relative astrometry was performed between the *Chandra* frames and those obtained at the VLT (see Section 2.3). Sources located in the *Chandra* frame were centroided by fitting Gaussian profiles to their light distributions. These were then compared with

the VLT Focal Reducer and low dispersion Spectrograph (FORS2)[1] frame (see Section 2.3.2), giving a total of six optical counterparts to X-ray sources in the optical image. An astrometric solution was computed with the IRAF task GEOMAP, which places the afterglow on the FORS2 frame with an accuracy of 0.45 arcsec. Subsequent relative astrometry between the FORS2 and *HST* Wide Field and Planetary Camera-2 (WFPC2) and Near Infrared Camera and Multi-Object Spectrometer (NICMOS) frames was performed using 10 (WFPC2, *F606W*) and seven (NICMOS, *F160W*) sources in common to each frame. The total error in the placement of the X-ray afterglow on the *HST* images is ∼0.5 arcsec. We additionally placed the afterglow on our other optical/IR frames (other *HST* filters and instruments, Gemini and *Spitzer* observations) by performing relative astrometry between NICMOS and those images, the resulting error on these transformations is typically very small (∼0.1 arcsec) and does not contribute significantly to the overall positional error budget.

2.3 Host galaxy

At the location of the X-ray afterglow we clearly find an extremely red host galaxy, with $g = 27.41 \pm 0.3$ and $K_s = 21.74 \pm 0.13$ (AB magnitude, see below for more details). The probability of a chance alignment of a $g \sim 27.5$ galaxy is moderate, even within our 0.5 arcsec error circle, with $P_{\rm chance} \sim 0.1$ following Bloom, Kulkarni & Djorgovski (2002) and Levan et al. (2007). However, the probability of an ERO is much lower, indeed, simply utilizing the *K*-band number counts (Conselice et al. 2008) and not accounting for the colours, would imply a probability of $P_{\rm chance} \leq 1$ per cent. Hence we identify this galaxy as the host of GRB 080207.[2] We have acquired deep observations of the host galaxy in 19 bands ranging from observed frame optical *B* band to submm 850 μm. The host galaxy is faint or undetected in the optical and bright at longer wavelengths, indicating very red colours not usually associated with GRB hosts. Various images of the field of the host galaxy are displayed in Fig. 3. The XRT position (large green circle) is unable to uniquely determine the host, while the improved *Chandra* position (small red circle) intersects three small knots with similar colours, which will be assumed to belong to the host galaxy system.

2.3.1 Hubble Space Telescope

The X-ray position of GRB 080207 was observed by the *HST* using both the WFPC2 in the *F606W*, *F702W* and *F814W* filters, the NICMOS with the NIC3 camera and *F160W* filter (*H* band) and the Wide Field Camera-3 (WFC3) with the *F110W* filter. Details of the individual observations are reported in Table 2.

The WFPC2 data were retrieved from the archive with 'on-the-fly' processing. The individual images were then cosmic ray rejected, shifted and combined via MULTIDRIZZLE to produce a final image with a scale of 0.06 arcsec pixel^{-1} (roughly 2/3 of the native pixel size).

NICMOS images were cleaned for quadrant-dependent residual bias levels (pedestal effect) using PEDSKY and subsequently processed through MULTIDRIZZLE on to an output grid with pixel size 0.1 arcsec. WFC3 observations were obtained with a standard four-point box dither pattern, and also combined via MULTIDRIZZLE, with the native pixel size unchanged (0.13 arcsec).

There is no evidence for host galaxy emission in any of the WFPC2 observations. However, the *F160W* observations clearly show evidence for a host galaxy at the location of the X-ray afterglow of GRB 080207. Point source limits for objects at the location of GRB 080207 in the WFPC2 images are $F606W = 26.8$, $F702W = 27.2$, $F814W = 27.0$ (all 3σ AB magnitude limits). However, the galaxy is clearly extended in the *F160W* observations, hence we attempt to derive more realistic limits using apertures equal to the half light radius of the galaxy as measured in the *F160W* observations (0.4 arcsec), and then assumed this accounted for only 50 per cent of the total galaxy light, hence brightening the limits by a factor of 2. In practice the true limiting magnitude depends on the distribution of light within the galaxy, where bright knots of emission could often be seen, even if low surface brightness areas were missed. However, these limits are broadly in agreement with the magnitude limits obtained by populating the images with fake sources of half light radii equal to that of the host, and subsequently attempting to recover them via SExtractor (Bertin & Arnouts 1996). The resulting limits are $F606W = 25.4$, $F702W = 25.65$ and $F814W = 25.02$ (see also Table 2).

2.3.2 Ground-based host observations

In addition to the optical and nIR observation with *HST*, deep imaging of the host galaxy was obtained with the VLT, Gemini and Keck.

The VLT *R*-band observation was carried out on 2008 April 1, using FORS2. In this image, the host galaxy remains undetected to a limit ∼25.65. Although the *R*-band limit is affected by blending with a neighbouring source, the limiting magnitude is broadly consistent with that from *HST*.

The Gemini imaging was obtained with the Gemini Multi-Object Spectrograph (GMOS) in the *z* band, and the Near Infrared Imager and Spectrometer (NIRI) in *J* and *K*. The seeing in the *z*-band observations was very good (∼0.5 arcsec), but was poorer for the *J* and *K* band (∼0.9 arcsec). These observations were reduced in the standard fashion under IRAF. The host is detected in each of these observations, although only with marginal significance in the *J*-band observations. Photometry of the host galaxy was performed relative to Sloan Digital Sky Survey (SDSS) observations of the field for the *z*-band observations, and in comparison to Two-Micron All Sky Survey (2MASS) for the *J* and *K*.

The Keck observations were performed with the Low Resolution Imaging Spectrometer (LRIS) in the *g* and *I* bands. The images were reduced with standard IRAF techniques and zero magnitudes were calibrated relative to SDSS stars in the field. We note that both the *g* and *I* bands are deeper than the *HST* and Gemini optical observations, resulting in a detection of the host at low wavelength indicating redshift $z < 2.8$. The K_s observations provided a factor of ∼2 better signal-to-noise ratio than the Gemini observations in the *K* band, and flux consistent within 1σ. The K_s band is calibrated using sources in the field common with the Gemini frame. See Table 2 for a full summary of all observation details and results.

2.3.3 Spitzer

The host of GRB 080207 was also observed by the *Spitzer Space Telescope*, utilizing both the Infrared Array Camera (IRAC) in all

[1] Although tying directly to the *Hubble Space Telescope* (*HST*) images would have been preferable, this is unfeasible due to the small field of view which contained too few sources in common.

[2] We note that while this paper was in review, a separate paper by Hunt et al. (2011) has appeared. Our precise position confirms their host identification, and their independent discovery of the ERO host.

four bands (3.6, 4.5, 5.8 and 8.0 μm) and with the Multiband Imaging Photometer (MIPS) at 24 μm. The host is clearly detected in all IRAC and MIPS bands, indicating significant nIR and mIR emission, possibly suggesting a massive and dusty host, respectively. The clear detections in these bands are in contrast to the majority of GRB hosts which are undetected (or very weakly detected) in similar observations (e.g. Le Floc'h et al. 2006; Castro Cerón et al. 2010). As the host is unresolved at the resolution of *Spitzer*, photometry of host was performed on the standard post-basic calibrated data (BCD) mosaics, utilizing small apertures (2.4 and 7.4 arcsec for IRAC and MIPS, respectively) and applying tabulated aperture corrections and zero-points. The resulting magnitudes are shown in Table 2.

2.3.4 SCUBA2

As a part of the early 'shared risk' operations with SCUBA2 (Holland et al. 2006; Economou et al. 2008) on the James Clerk Maxwell Telescope (JCMT), we obtained ∼43 min of observations in the 450 and 850 μm bands during the nights 2010 February 25, 2010 February 26 and 2010 March 12. The imaging was carried out in the SCAN mode with a DAISY scanning pattern. The data were reduced using the STARLINK module SMURF, running MAKEMAP in the iterative mode[3] to map the SCAN data into a sky image with a pixel scale of 3 arcsec (e.g. Jenness et al. 2011). The sky maps are flux calibrated relative to the submm flux of CRL 618 which was observed during the same nights as the science observations (e.g. Dempsey et al. 2010). Before the maps for all nights were co-added, astrometric corrections were applied as determined by separate observations of pointing sources obtained during each night. We performed aperture photometry in the 450 and 850 μm bands, respectively – measuring fluxes $23\,037 \pm 17\,740$ and 2529 ± 4374 μJy, respectively, although the host is undetected. Using blank apertures on the map we estimate 3σ limiting magnitudes of 12.1 and 13.6 (AB magnitudes) in the 450 and 850 μm bands, respectively, which offer only weak constraints on the submm emission.

3 AFTERGLOW PROPERTIES

The X-ray spectrum exhibits apparent absorption significantly in excess of the Galactic value. The preferred zero redshift model results in $N_{\rm H} \sim 75 \times 10^{20}\,{\rm cm}^{-2}$ (cf. total Galactic $N_{\rm H}$ column $\sim 1.94 \times 10^{20}\,{\rm cm}^{-2}$) with $\chi^2/{\rm dof} = 125/153$. Attempting to fit a broken power law with fixed $\Delta\beta = 0.5$, e.g. assuming the spectral turnover to be influenced by a cooling break in the X-ray band, results in significantly worse fits with $\chi^2/{\rm dof} = 168/152$ and 36/29, respectively, for PC and WT mode data, suggesting that excess $N_{\rm H}$ is the most likely explanation for the observed spectrum.

Grupe et al. (2007) suggest that the X-ray measured $N_{\rm H}$ column can be used to limit the redshift by

$$\log(1+z) < 1.3 - 0.5\,\log_{10}(1+\Delta N_{\rm H}), \qquad (2)$$

where $\Delta N_{\rm H}$ is the difference between Galactic and observed $N_{\rm H}$ values in units of $10^{20}\,{\rm cm}^{-2}$, fitted at zero redshift. This would suggest that GRB 080207 originates from $z < 1.3$. Interestingly the only GRB in the sample of Grupe et al. (2007) to be found with a higher $N_{\rm H}$ than GRB 080207 is GRB 051022, whose optical afterglow was also markedly suppressed (Rol et al. 2007; ?). Indeed, although it is commonly very difficult to assess the redshifts for dark GRBs it is occasionally possible to pinpoint redshifts for bursts whose optical afterglows are somewhat suppressed, and are invisible to UVOT, but are still visible to deep ground-based optical observations. In these cases the measured (rest frame) column densities are apparently higher than those for the GRBs with very bright optical afterglows (Schady et al. 2007).

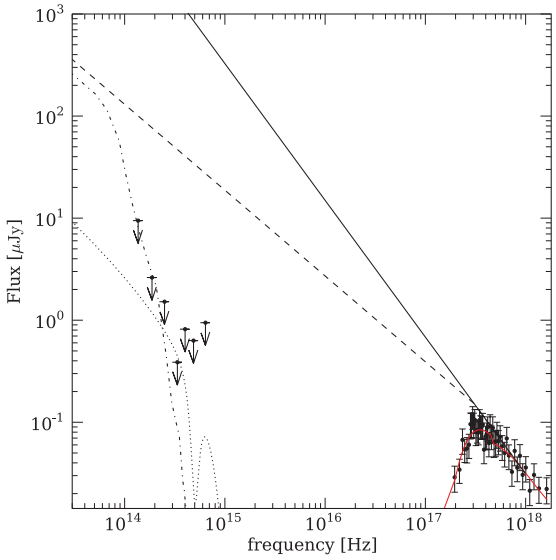

Figure 2. The afterglow SED ∼11 h post-burst, ranging from nIR to X-ray frequencies. The solid red line shows the X-ray model fitted with redshift $z = 1.74$, the solid black line is the X-ray power law extrapolated without a spectral break and the dashed line with a $\Delta\beta = 0.5$ cooling break. The power law and spectral break model is shown absorbed in the rest frame by a MW reddening law with $A_V = 2.6$ (dotted line), and by a SMC law with $A_V = 3.7$ (dash–dotted line).

Assuming that GRB 080207 is *not* limited to $z < 1.3$, we fit the X-ray spectrum with single power-law model absorbed by the Galactic $N_{\rm H}$ column *and* an absorber redshifted to $z = 1.74$ as suggested by out photometric redshift solutions for the host (see Section 4.1). This model suggests an X-ray spectral slope $\beta = 1.34^{+0.17}_{-0.16}$ and a significantly higher $N_{\rm H}$ column than the zero redshift case with $N_{\rm H} = 679^{+125}_{-114} \times 10^{20}\,{\rm cm}^{-2}$. This makes this one of the highest measured rest-frame $N_{\rm H}$ column of any GRB host yet.

Extrapolating the X-ray power law to optical/nIR frequencies and re-normalizing the integrated flux to be consistent to the 11 h post-burst flux suggested by the light curve reveals the optical/nIR flux limits are fainter than expected. The X-ray-to-optical spectral slope is estimated to be $\beta_{\rm OX} < 0.3$ and thus this burst fulfil the criteria for dark bursts of Jakobsson et al. (2004) (and also fulfils the dark criterion by van der Horst et al. 2009 since $0.3 < \beta_{\rm X} - 0.5$). To evaluate an optical extinction that explains the optical darkness of this burst, we adopt extinction curves derived for the Milky Way (MW; Seaton 1979) with $R_V = 3.1$, the Small Magellanic Cloud (SMC; Prevot et al. 1984) with $R_V = 2.72$, typical starburst galaxies (SB; Calzetti et al. 2000) with $R_V = 4.05$ and the afterglow of the dark GRB 080607 (Perley et al. 2011).

The afterglow model SED is reddened after extrapolating the X-ray into the optical–nIR regime, and after introducing a cooling break with $\Delta\beta = 0.5$ shortwards of the XRT band (Fig. 2). By requiring that the absorbed extrapolation falls below the detection limits, at the redshift $z = 1.74$ a rest-frame line-of-sight extinctions in excess of 2.6 mag (MW), 3.7 mag (SMC), 4.1 mag (SB) and 3.4 mag (GRB 080607) is found. These all suggest that the optical

[3] I.e. iteratively fitting detector signal and background noise.

Table 1. *Chandra* X-ray position and fitted parameters for the afterglows analysis. The quoted hydrogen column and extinction are calculated in the rest frame of the hosts photometric redshift ($z_{\rm phot} = 1.74$).

Afterglow properties	
RA, Dec. (J2000)	13:50:02.98, +07:30:07.4
Error box	0.5 arcsec
χ^2/dof (spectral fit)	48.49/48 $\sim$ 1.01
β	$1.34^{+0.17}_{-0.16}$
$N_{\rm H}$	$679^{+125}_{-114} \times 10^{20}$ cm^{-2}
A_V (MW law)	$\geq$2.6
A_V (GRB 080607 law)	$\geq$3.4
A_V (SMC law)	$\geq$3.7
A_V (SB law)	$\geq$4.1
χ^2/dof (light curve)	65.78/66 $\sim$ 1.00
α	1.7 ± 0.1

extinction is indeed also very high compared to the bulk GRB population, but that the dust-to-gas ratio is comparable to that found in other hosts (e.g. Perley et al. 2009; Schady et al. 2010). A summary of derived afterglow properties can be found in Table 1.

4 HOST GALAXY PROPERTIES

The g-band detection of the host galaxy suggests that it lies below $z \sim 4$. Coupled with the relatively bright magnitudes in the nIR to mIR, and the red colours across the whole of the wavelength range, rather than a sharp break in the optical and a flat SED in the optical–nIR, the favoured interpretation is that of a dusty sightline. This is also strongly indicated by the detection of the host galaxy at 24 μm, and although the SCUBA2 limits are not deep enough to offer any significant constraints, they are fully consistent with submm dust emission at the photometric redshift $z \sim 1.7$ we derive in Section 4.1.

The observed lower limit on the colour of $R - K > 5.4$ (equivalent to $R - K > 3.7$ in AB magnitudes) is one of the reddest GRB hosts yet discovered, and indicates that, at least in the case of GRB 080207, the environment is markedly different to that of optically bright bursts. The high-resolution imaging acquired by the WFC3 on *HST* resolves the large-scale structure of the host, which is displaying an irregular morphology, suggesting a merging or disturbed system, possibly crossed by dust lanes.

In the following section we will discuss the photometric redshift solutions and the rest-frame properties which it implies. The 19 bands covered by photometry are presented in Table 2 and a five-band mosaic image in Fig. 3 shows the host going from non-detected in the visual, to faint in z-band to strong detections in nIR J band and IR 4.5 μm. In the following we have assumed a Λ cold dark matter (ΛCDM) cosmology with $\Omega_{\rm M} = 0.27$, $\Omega_\Lambda = 0.73$ and $H_0 = 71$ km s^{-1} Mpc^{-1}.

4.1 Photometric redshift

The 19-band observations cover a broad wavelength range from optical to submm, and should allow a well constrained photometric redshift to be determined, and estimates of the physical properties (e.g. mass and SFR) of the host galaxy to be made without relying on extrapolating an assumed spectral shape. To enable detailed and accurate modelling of a system that could possibly contain both a young and starbursting stellar population and an older, redder component we find that allowing for a linear combination of two templates provide a significantly better fit than only using a single template. Hence, to simultaneously fix the photometric redshift and the full rest-frame SED, we fitted a linear combination of two templates: one coming from a set of detailed optical templates including models described in Coleman, Wu & Weedman (1980) and

Table 2. Photometric observations of the GRB 080207 host galaxy as part of this work. Magnitudes are in the AB system. Limits in the magnitude column are 3σ estimated from half-light radius apertures (WFPC2) or point source limits (SCUBA2). In the flux column, the actual flux measured in the aperture also in the cases of non-detections are reported.

Host observation log					
Date	Instrument	Filter	Exp. time (s)	Magnitude (AB)	flux (μJy)
2009-02-19	Keck/LRIS	*g*	1640	27.41 ± 0.3	0.04 ± 0.01
2008-03-18	*HST*/WFPC2	*F606W*	1600	>25.4	0.16 ± 0.10
2008-04-01	VLT/FORS2	*R*	2000	>25.65[a]	0.14 ± 0.07
2009-03-21	*HST*/WFPC2	*F702W*	3600	>25.65	0.2 ± 0.08
2009-02-19	Keck/LRIS	*I*	1500	25.84 ± 0.29	0.17 ± 0.05
2009-03-20	*HST*/WFPC2	*F814W*	3300	>25.03	0.38 ± 0.13
2009-02-24	Gemini/GMOS	*z*	1260	25.02 ± 0.25	0.18 ± 0.05
2009-02-19	Gemini/NIRI	*J*	2880	23.87 ± 0.31	1.06 ± 0.35
2009-12-10	*HST*/WFC3	*F110W*	2400	23.32 ± 0.09	1.75 ± 0.17
2008-04-05	*HST*/NICMOS	*F160W*	2560	23.04 ± 0.14	2.27 ± 0.34
2009-02-19	Gemini/NIRI	*K*-prime	2880	21.94 ± 0.24	6.25 ± 1.62
2009-05-31	Keck/NIRC	*K*-short	1500	21.74 ± 0.13	7.52 ± 0.93
2009-03-20	*Spitzer*/IRAC	3.6 μm	1600	20.81 ± 0.04	17.7 ± 0.76
2009-03-20	*Spitzer*/IRAC	4.5 μm	1600	20.67 ± 0.03	20.14 ± 0.65
2009-03-20	*Spitzer*/IRAC	5.8 μm	1600	20.21 ± 0.13	30.76 ± 4.32
2009-03-20	*Spitzer*/IRAC	8.0 μm	1600	20.63 ± 0.19	20.89 ± 4.29
2008-07-31	*Spitzer*/MIPS	24 μm	5407	18.50 ± 0.20	148.59 ± 32.1
2010-02-25,26, 03-12	JCMT/SCUBA2	450 μm	2616	>12.1	$23\,040 \pm 17\,740$
2010-02-25,26, 03-12	JCMT/SCUBA2	850 μm	2616	>13.6	2530 ± 4370

[a]Indicates blending with a nearby source affects the limiting magnitude.

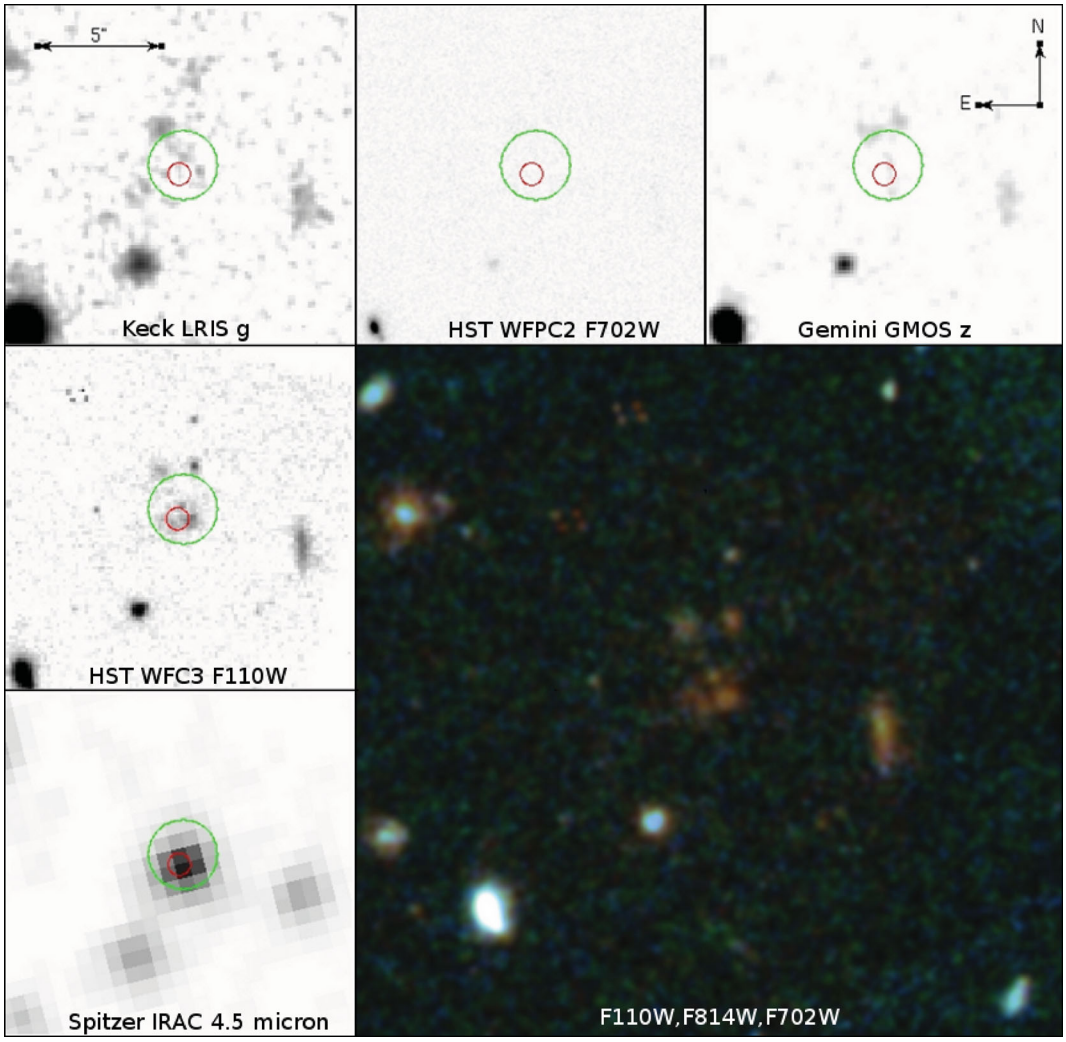

Figure 3. Five-band mosaic image of the field of GRB 080207 including its host galaxy (top and left-hand panels). The red circle marks the *Chandra* X-ray position and error box, the green circle shows the *Swift*/XRT position and error box. The host is faint or undetected in the optical but shows strong emission in nIR and longer wavelengths. The large lower right-hand panel shows a three-filter false colour image showing the extremely red host galaxy in the centre and a number of other red galaxies also in the field.

Bruzual & Charlot (1993); and the second set of templates (described by Siebenmorgen & Krügel 2007) containing galaxies with significant amounts of dust increasing their IR and submm luminosities by reprocessing the UV and optical light. Furthermore, we fitted the reddening of the first set of models by assuming a Calzetti et al. (2000) reddening law. The dusty templates in the second set already include a dust screen model, and are not reddened any further. In total this comprises six free parameters (redshift, A_V, two templates and two normalization constants.), and for 19 photometry data points gives dof $= 19 - 6 = 13$.

Fitting the available photometry, including measured fluxes for the non-detections, and allowing both redshift and host absorption to vary as free parameters (see Svensson et al. 2010) yield a primary photometric redshift solution of $z = 1.74^{+0.06}_{-0.05}$ with χ^2/dof $=$ 19.37/13 $\sim$ 1.49, shown in Fig. 4. The redshift error is the central 1σ interval, i.e. the integrated probabilities above and below the interval are both $(1 - 0.683)/2$. This confidence interval is relatively narrow, but somewhat broader at 2σ, providing $z = 1.74^{+0.34}_{-0.18}$. This result is broadly consistent with an independently derived solution with HYPERZ (Bolzonella, Miralles & Pelló 2000) using only the optical and nIR photometry. It is also broadly consistent at the $\sim$1.5σ level, with the $z = 2.2^{+0.2}_{-0.3}$ obtained by Hunt et al. (2011), using a smaller data set. We do not attempt to increase the errors due to possible systematic offsets between different instruments, however, note that this would not change our photometric redshift, but (for modest additional errors) would simply slightly increase the confidence ranges. It is also worth noting that a higher redshift than provided by the best fit would further increase the rest-frame hydrogen column derived from the X-ray spectrum, e.g. $\sim$10 per cent higher at $z = 2.2$. A significantly higher solution is effectively ruled out by the *g*-band detection.

4.2 Rest-frame properties of the host

The rest-frame properties of the host galaxy as derived from these fits are shown in Table 3. We estimated physical galactic properties from the rest-frame *k*-corrected and extinction-corrected SED. Stellar mass content is estimated from the rest-frame *K*-band absolute magnitude (Savaglio, Glazebrook & Le Borgne 2009), corresponding to between IRAC 5.8 and 8 μm at $z = 1.74$. For the SFR we make two estimates, one based on the *U*-band luminosity (Cram et al. 1998) and other based on the far-infrared (fIR) luminosity

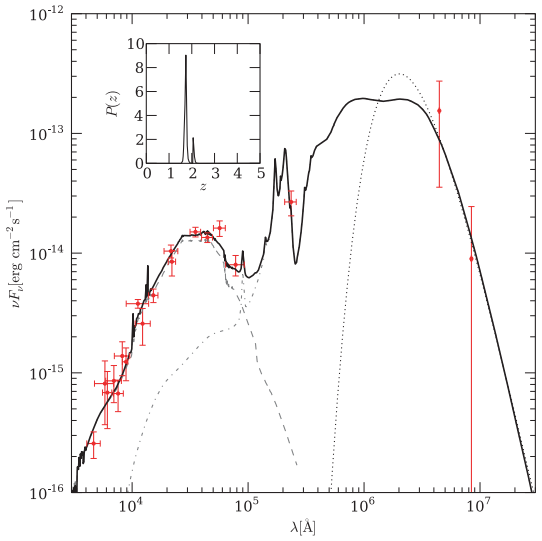

Figure 4. The host galaxy SED and photometric redshift solutions at $z_{\rm phot} = 1.74^{0.06}_{-0.05}$. The wavelength scale is in the observer frame. The thick solid line shows the composite template model with the dashed, and dash–dotted lines showing the individual components. The dotted line is purely thermal emission from $\sim 7 \times 10^8\,{\rm M}_\odot$ dust at ∼45 K. The inset figure shows the probability distribution as a function of redshift. Errors are 1σ.

Table 3. Rest-frame properties of the hosts SED template fit. Absolute magnitudes are not corrected for host extinction. Stellar mass and SFRs are corrected for a host internal extinction of $A_V = 1.9$. The quoted errors are 1σ statistical errors on the best-fitting template.

Host rest-frame properties	
$z_{\rm phot}$	$1.74^{+0.06}_{-0.05}$
χ^2/dof	19.37/13 ∼ 1.49
A_V	∼1.9
M_U	-20.29 ± 0.04
M_B	-20.99 ± 0.04
M_V	-21.86 ± 0.04
M_K	-23.89 ± 0.04
$L_{\rm fIR}$	$2.4 \pm 0.09 \times 10^{12}\,{\rm L}_\odot$
$\log_{10}(M_\star/{\rm M}_\odot)$	11.05 ± 0.02
${\rm SFR}_U$	$40.7 \pm 1.6\,{\rm M}_\odot\,{\rm yr}^{-1}$
${\rm SFR}_{\rm fIR}$	$416 \pm 17.0\,{\rm M}_\odot\,{\rm yr}^{-1}$

(Kennicutt 1998). The host is massive and rapidly star forming – assuming that the fIR traces the true SFR more accurately than the U band. Placing it on the SFR/M_* versus M_* plane compared to the bulk GRB hosting galaxy population (e.g. Castro Cerón et al. 2006, 2010; Savaglio et al. 2009) suggests that it is one of the most massive and most actively star-forming GRB hosts to date. From the SED model we estimate a rest-frame fIR luminosity $L_{\rm fIR} \sim 3 \times 10^{12}\,{\rm L}_\odot$ suggesting that GRB 080207 is one of few bursts with a ultraluminous infrared galaxy (ULIRG) host (Michałowski et al. 2008). However, it should be noted that the ULIRG classification rests mainly on the 24 μm MIPS detection, and while the SCUBA2 limits are consistent, they are also too bright to offer significant constraints on the fIR nature of the SED.

Comparing the host with the luminosity function at $z \sim 2$ (e.g. Dahlen et al. 2005, 2007) suggests that it is comparable to the characteristic luminosity in the B band; $L_B \sim 1.3 L_B^*$, in contrast to the typically underluminous properties of optically bright GRB selected samples.

In particular, it is clear that the host extinction in this case is high in comparison to the bulk GRB population – the dominant model in the optical has an $A_V \sim 1.9$ while the second component has a total of ∼100 mag of extinction from core to surface (see Siebenmorgen & Krügel 2007 for a description of their dust model) – suggestive of a major dust content within the host. Although a 3σ detection is lacking from SCUBA2, we estimate a 3σ upper limit of the dust mass as ~ 1.2–$1.4 \times 10^9\,{\rm M}_\odot$ assuming a dust temperature of 45 K (e.g. Michałowski et al. 2008), and also note that a lower temperature would increase the necessary dust mass. The possibility of significant dust content is in contrast to the majority of GRB host galaxies, whose photometry suggests relatively little dust (e.g. Tanvir et al. 2004; Savaglio et al. 2009), indeed it is more similar to that commonly found in submm-selected galaxies (e.g. Michałowski, Hjorth & Watson 2010a). However, it should be noted that these studies have mainly concerned host samples optically selected, and *may not* be representative of the true population.

5 DISCUSSION

5.1 Implications for dark GRBs

GRB 080207 (see also Hunt et al. 2011) is one of very few GRB hosts which can be classified as an ERO. The other examples GRBs 030115 (Levan et al. 2006a) and 020127 (Berger et al. 2007) also host bursts which were dark, or showed significant extinction in their afterglow light curve. Several other bursts also show very red colours in their afterglows, indicating significant extinction along the line of sight (e.g. Tanvir et al. 2008), however, at least in some cases where the afterglow is unusually red, observations of the host galaxies do not reveal exclusively red colours (e.g. Djorgovski et al. 2001; Gorosabel et al. 2003a,b; Rol et al. 2007; Jaunsen et al. 2008; Perley et al. 2009), although there is an apparent trend for the dark GRB host population to include much redder galaxies than that of the optically bright population (e.g. Hashimoto et al. 2010; Küpcü Yoldaş et al. 2010). Indeed, GRB hosts in general are very blue and typically subluminous (Le Floc'h et al. 2003; Christensen, Hjorth & Gorosabel 2004), suggesting that only a relatively small fraction of GRB-selected star formation is obscured – at least so far as the bulk GRB hosting population is represented by bursts with optically bright afterglows. Further the blue colours of the GRB hosts, and the relatively low detection rate at long wavelength (e.g. Berger et al. 2003; Tanvir et al. 2004) in the pre-*Swift* sample suggest that few GRB hosts are dusty systems, in contrast to submm observations operating in a similar redshift range, which suggest that the bulk of star formation is obscured, with a good fraction occurring in ULIRG-like galaxies (Chapman et al. 2005; Michałowski et al. 2010a).

At first sight then it would appear that the complete set of galaxies hosting GRBs are very different from those of submm galaxies, although the direct comparison is far from trivial (e.g. Watson et al. 2004). Indeed, when comparing the rate of submm detections with that expected under simple models of paucity, submm bright GRB hosts are only marginally (∼2σ) below the expected values (Tanvir et al. 2004; Le Floc'h et al. 2006). Though it should be noted that the sample of submm observations of hosts is relatively small, and that this host sample had a median redshift ∼1.2 compared

to the median redshift of submm galaxies ∼2.2 (Chapman et al. 2005).

An alternative approach is to study the optical/IR properties of both GRB hosts and submm galaxies. The median $I - K$ colour of submm-selected galaxies is $I - K = 4.1 \pm 0.2$ (Smail et al. 2004), much redder than the general field population which has median $I - K = 2.8 \pm 0.1$ (Smail et al. 2004). In contrast the GRB population is typically very blue (if somewhat heterogeneously selected to date), with mean colours for optically bright bursts of $I - K = 1.6 \pm 0.3$, based on the sample of Savaglio et al. (2009), although a significant fraction of GRB hosts are undetected in deep K-band observations, implying at times even bluer colours.

The mean ratio of [N II]/Hα in submm galaxies at $z \sim 2$ is of order 0.5 based on deep IR spectroscopy (Swinbank et al. 2004), in contrast the (relatively local) GRB hosts with the same measure yield [N II]/Hα $\sim$ 0.1 (Savaglio et al. 2009; Levesque et al. 2010b). This suggests that even at $z \sim 2$, where the universal metallicity may have dropped significantly, submm bright galaxies may not be the most promising locations for GRBs. Indeed, the highest [N II]/Hα ratio in the optically bright GRB sample of ∼0.2 would only include approximately ∼20 per cent of the submm sample of Swinbank et al. (2004) as shown in Fig. 5. Although few hosts of dark bursts have direct measurements of their metallicities, making a direct comparison difficult, we note that the dark GRB 020819 has the highest measured [N II]/Hα so far reported (Levesque et al. 2010a), suggesting the corresponding distribution for dark bursts includes metallicities at least ∼× 2 higher. Future observations of the [N II]/Hα ratio in GRB hosts at higher z (for example in the IR with X-shooter), should enable firm statistical statements to be made. In the meantime, we can discuss the host mass distribution which provides a rough proxy for the metallicity distribution.

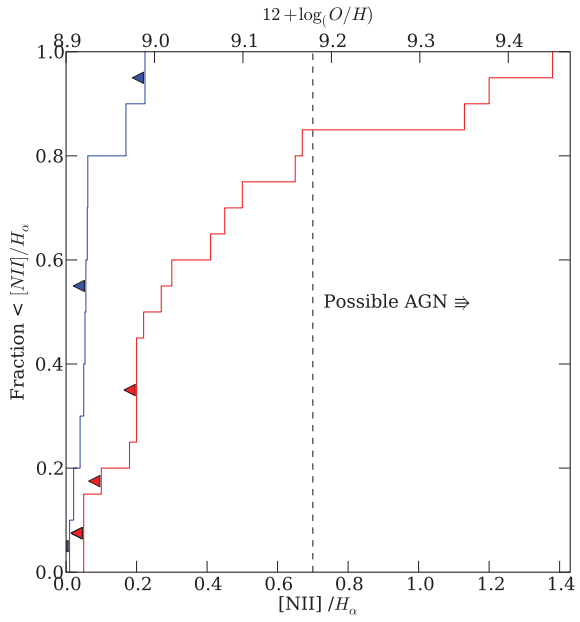

Figure 5. Cumulative distributions of the [N II]/Hα ratio for low-redshift ($z < 0.7$), optically bright GRB hosts (blue) in comparison to $z \sim 2$ submm galaxies (red). Triangles indicate upper limit measurements. Submm galaxies with [N II]/Hα > 0.7 may have active galactic nucleus (AGN) contribution. All galaxies with Hα rest-frame FWHM < 1000 km s^{-1} from Swinbank et al. (2004) have been included.

Table 4. Stellar masses of all host galaxies of dark bursts available to date. Note that in the case of GRB 090417B we have supplemented the existing data with additional photometry and derived new stellar mass estimates.

GRB	z	$\log_{10}(M_*/M_\odot)$	Ref. (mass or photometry)
970828	0.958	9.57	Svensson et al. (2010)
000210	0.846	9.21	Svensson et al. (2010)
020819	0.41	10.52	Svensson et al. (2010)
050223	0.59	9.81	Svensson et al. (2010)
051022	0.807	10.49	Svensson et al. (2010)
060210	3.9	10.56	Perley et al. (2009)
061126	1.16	11.16	Svensson et al. (2010)
061222	2.08	7.65	Perley et al. (2009)
080207	1.74	11.05	This paper
080325	2	10.85	Hashimoto et al. (2010)
080607	3.036	11.88	Chen et al. (2010)
090417B	0.3	9.25	Holland et al. (2010)

5.2 The mass distribution of dark burst hosts

In order to further understand the relations between the dark burst hosting galaxy population and ULIRG/submm-like galaxies, we compare the stellar mass distributions of submm galaxies calculated by Michałowski et al. (2010a) and Michałowski, Watson & Hjorth (2010b) with the stellar masses of dark burst hosts (see Table 4) and the optically bright bursts to redshift $z < 4$. We also estimate the submm galaxy masses with our own SED fitting code, and note that results are consistent with the adopted values. The cumulative mass distributions are shown in Fig. 6. While it is important to note that the host sample of dark GRBs consists of only 11 galaxies, the results clearly show that dark bursts are systematically hosted by the most massive systems compared the optically bright GRBs. The formal probability that the samples of optically dark and optically bright bursts are drawn from the same population is given by the Kolmogorov–Smirnov (KS) test, where $P_{\rm KS} = 0.009$. The contrasting host masses between optically bright and dark bursts is particularly interesting as it lends further credibility to claims that samples based primarily on bursts with optically detected

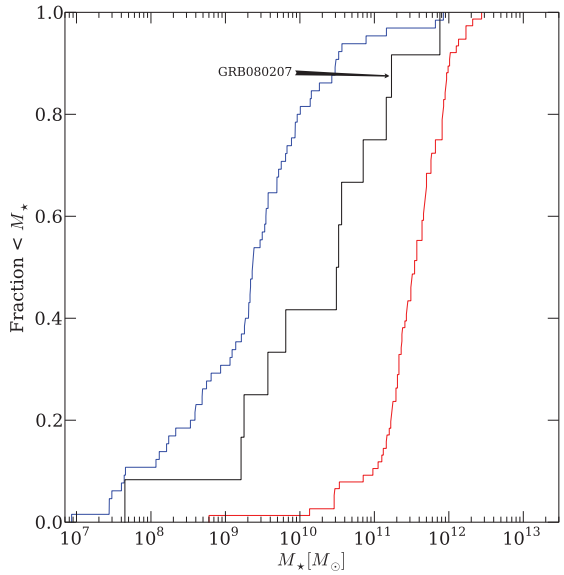

Figure 6. Cumulative distribution of stellar mass in optically bright GRB host galaxies (blue line) and hosts of dark bursts (black line). For a comparison we also show the distribution of stellar masses of the submm galaxies (red line) calculated by Michałowski et al. (2010a,b).

afterglows could be severely inhibited by selection effects (e.g. Fynbo et al. 2009).

Although we have not been able to reach a detection of the host submm flux by SCUBA2, the number of GRB hosts with significant dust content can roughly estimated. Assuming that some fraction of dark bursts occur in obscured systems, and also have similar dust to mass ratios – we compare their stellar mass distributions in Fig. 6. Roughly estimated, ∼90 per cent of the dark burst hosts are more massive than the least massive submm galaxy – and hence under this simple argument one could expect a similar detection rate of dark GRB hosts in the submm at SCUBA sensitivity. Depending on the intrinsic mass function of the submm population, even greater detection rates could be plausible with SCUBA2 and even with short integrations with ALMA when considering that the submm galaxy sample in this comparison is flux limited (Chapman et al. 2005). In terms of physical properties of the dark burst hosts, this suggests that dark bursts are hosted predominantly by a very dust-rich galaxy population.

Given that GRBs trace (at best) a fraction of star formation, potentially even at moderately large redshift it is surprising that attempts to transfer directly between GRB rate and SFR produce even moderately consistent results (e.g. Price & Schmidt 2004; Yüksel et al. 2008; Kistler et al. 2009). Although the sample of dark bursts to date with detected and studied host galaxies is still small, the emerging picture suggests that they indeed trace a different galaxy population than the optically bright sample. Certainly the host of GRB 080207 is more akin to submm or ULIRGs than to the typical GRB hosts, suggesting that it is part of a subset of the GRB hosting galaxy population that trace star formation in more massive, dusty and metal-rich environments. In the face of the growing evidence that dark bursts can be hosted at higher metallicity than the bulk GRB population studied today, it should be considered likely that GRBs can offer significant advantage over other methods to study the evolution of the cosmic star formation history – but only by paying due attention to sample selection effects and understanding the dark burst host population to avoid bias effects.

Although there is no direct measurement of the metallicity of the host of GRB 080207, the high stellar mass is suggestive of a metal-enriched environment – again raising the question of what is the nature and metallicity dependence of GRB progenitors? Considering the low metallicities typically associated with the bulk of the GRB hosts, we note that several authors (e.g. Levan, Davies & King 2006b; Davies et al. 2007) have discussed tight binary systems as possible progenitors to GRBs in high-metallicity environments. While this would still require ongoing star formation and high-mass stars, Habergham, Anderson & James (2010) report evidence for top-heavy initial mass functions (IMFs) in merging systems, increasing the likelihood of a GRB progenitor.

If the galaxy hosting GRB 080207 is undergoing a merger that further increased its rate of forming massive stars, and if a binary progenitor is indeed possible at high metallicity – maybe massive and dust-rich galaxies are hosting a non-negligible fraction of bursts. Although to which extent these conclusions can be generalized to other dark bursts is far from certain.

6 SUMMARY

We have studied the afterglow of the dark GRB 080207 from X-ray to nIR wavelengths and presented evidence of significant extinction in excess of at least 2.6 mag (MW law) in the rest-frame visual as the cause of its optical–nIR darkness. The high optical extinction is also echoed by the rest-frame hydrogen column which is the highest measured in any GRB environment to date. Lacking optical detection of the afterglow we have used observations of the X-ray afterglow at late time with *Chandra*, enabling an X-ray position to accurately identify the host galaxy. The ERO host SED has been studied in 19 bands from optical to submm allowing us to estimate a photometric redshift ∼1.74 and an average optical extinction of $A_V \sim 1.9$ in a massive galaxy. Furthermore, the host appears to be a ULIRG from its fIR SED, with a high SFR as traced by the fIR light. With a significant fraction of all bursts being classified as dark, and an increasing desire to utilize GRBs as high-redshift probes of the star formation evolution, the understanding of the nature of dark bursts should be highlighted. This, and a number of other dark bursts in similar hosts should further encourage the study of dark bursts, their host environments and how they relate to the evolving rate of star formation.

ACKNOWLEDGMENTS

We thank the referee for a careful review of this manuscript, which has substantially improved the paper. We thank Harvey Tannenbaum and the CXO staff for their help is securing rapid *Chandra* observations. KMS is grateful to the University of Warwick for doctoral studentship. AJL thanks STFC for post-doctoral fellowship. NRT is grateful to STFC for senior fellowship award. SBC acknowledges generous support from Gary and Cynthia Bengier and the Richard and Rhoda Goldman fund. PJ acknowledges support by a Marie Curie European Reintegration Grant within the 7th European Community Framework Program, and a Grant of Excellence from the Icelandic Research Fund. The Dark Cosmology Centre is funded by the DNRF. Based on observations made with the NASA/ESA *Hubble Space Telescope*, obtained from the data archive at the Space Telescope Institute. STScI is operated by the association of Universities for Research in Astronomy, Inc., under the NASA contract NAS 5-26555. The observations are part of proposal number 11343. This work is based in part on observations made with the *Spitzer Space Telescope*, which is operated by the Jet Propulsion Laboratory, California Institute of Technology under a contract with NASA. Based on observations made with ESO Telescopes at the La Silla or Paranal Observatories under programme 177.A-0591. This research has made use of data obtained from the *Chandra* Data Archive. This work made use of data supplied by the STFC funded UK *Swift* Science Data Centre at the University of Leicester. This paper made use of data products from the JCMT Science Archive (JSA) project. The JSA is a collaboration between the JCMT and the Canadian Astronomy Data Center (CADC). The JCMT is operated by the Joint Astronomy Centre on behalf of the Science and Technology Facilities Council of the United Kingdom, the Netherlands Organisation for Scientific Research and the National Research Council of Canada. The CADC is operated by the National Research Council of Canada with the support of the Canadian Space Agency.

REFERENCES

Berger E., Cowie L. L., Kulkarni S. R., Frail D. A., Aussel H., Barger A. J., 2003, ApJ, 588, 99
Berger E., Fox D. B., Kulkarni S. R., Frail D. A., Djorgovski S. G., 2007, ApJ, 660, 504
Bertin E., Arnouts S., 1996, A&AS, 117, 393
Blain A. W., Smail I., Ivison R. J., Kneib J.-P., 1999, MNRAS, 302, 632
Bloom J. S., Kulkarni S. R., Djorgovski S. G., 2002, AJ, 123, 1111
Bolzonella M., Miralles J.-M., Pelló R., 2000, A&A, 363, 476
Bouwens R. J., Illingworth G. D., Blakeslee J. P., Franx M., 2006, ApJ, 653, 53
Bouwens R. J. et al., 2009, ApJ, 705, 936
Bruzual A. G., Charlot S., 1993, ApJ, 405, 538

Bunker A. J. et al., 2010, MNRAS, 409, 855
Calzetti D., Armus L., Bohlin R. C., Kinney A. L., Koornneef J., Storchi-Bergmann T., 2000, ApJ, 533, 682
Castro Cerón J. M., Michałowski M. J., Hjorth J., Watson D., Fynbo J. P. U., Gorosabel J., 2006, ApJ, 653, L85
Castro Cerón J. M., Michałowski M. J., Hjorth J., Malesani D., Gorosabel J., Watson D., Fynbo J. P. U., 2010, ApJ, 721, 1919
Castro-Tirado A. J. et al., 2007, A&A, 471, 101
Cenko S. B. et al., 2009, ApJ, 693, 1484
Chapman S. C., Blain A. W., Smail I., Ivison R. J., 2005, ApJ, 622, 772
Chen H. et al., 2010, ApJ, 723, 218
Christensen L., Hjorth J., Gorosabel J., 2004, A&A, 425, 913
Coleman G. D., Wu C.-C., Weedman D. W., 1980, ApJS, 43, 393
Conselice C. J., Bundy K., Vivian U., Eisenhardt P., Lotz J., Newman J., 2008, MNRAS, 383, 1366
Cram L., Hopkins A., Mobasher B., Rowan-Robinson M., 1998, ApJ, 507, 155
Cucchiara A. et al., 2011, ApJ, 736, 7
Dahlen T., Mobasher B., Somerville R. S., Moustakas L. A., Dickinson M., Ferguson H. C., Giavalisco M., 2005, ApJ, 631, 126
Dahlen T., Mobasher B., Dickinson M., Ferguson H. C., Giavalisco M., Kretchmer C., Ravindranath S., 2007, ApJ, 654, 172
Davies M. B., Levan A. J., Larsson J., King A. R., Fruchter A. S., 2007, in Axelsson M., Ryde F., eds, AIP Conf. Ser. Vol. 906, Millimeter, Submillimeter and far Infrared Detectors and Instrumentation for Astronomy. Am. Inst. Phys., New York, p. 69
Dempsey J. T., Friberg P., Jenness T., Bintley D., Holland W. S., 2010, in Holland W. S., Zmuidzinas J., eds, Proc. SPIE Vol. 7741, Millimeter, Submillimeter, and Far-Infrared Detectors and Instrumentation for Astronomy V. SPIE, Bellingham, 77411x
Djorgovski S. G., Frail D. A., Kulkarni S. R., Bloom J. S., Odewahn S. C., Diercks A., 2001, ApJ, 562, 654
Economou F., Jenness T., Chrysostomou A., Cavanagh B., Redman R., Berry D. S., 2008, in Argyle R. W., Bunclark P. S., Lewis J. R., eds, ASP Conf. Ser. Vol. 394, Astronomical Data Analysis Software and Systems XVII. Astron. Soc. Pac., San Francisco, p. 450
Evans P. A. et al., 2007, A&A, 469, 379
Evans P. A. et al., 2009, MNRAS, 397, 1177
Fox D. W., Frail D. A., 2002, GRB Coordinates Network, 1250, 1
Fruchter A. S. et al., 2006, Nat, 441, 463
Fugazza D., D'Elia V., D'Avanzo P., Covino S., Tagliaferri G., 2008, GRB Coordinates Network, 7293, 1
Fynbo J. P. U. et al., 2009, ApJS, 185, 526
Gorosabel J. et al., 2003a, A&A, 400, 127
Gorosabel J. et al., 2003b, A&A, 409, 123
Greiner J. et al., 2009, ApJ, 693, 1610
Greiner J. et al., 2011, A&A, 526, A30
Groot P. J. et al., 1998, ApJ, 493, L27
Grupe D., Nousek J. A., vanden Berk D. E., Roming P. W. A., Burrows D. N., Godet O., Osborne J., Gehrels N., 2007, AJ, 133, 2216
Habergham S. M. et al., 2010, ApJ, 717, 342
Haislip J. B. et al., 2006, Nat, 440, 181
Hashimoto T. et al., 2010, ApJ, 719, 378
Hjorth J. et al., 2003, Nat, 423, 847
Hogg D. W., Fruchter A. S., 1999, ApJ, 520, 54
Hogg D. W., Pahre M. A., McCarthy J. K., Cohen J. G., Blandford R., Smail I., Soifer B. T., 1997, MNRAS, 288, 404
Holland W. et al., 2006, in Zmuidzinas J., Holland W. S., Withington S., Duncan W. D., eds, Proc. SPIE Vol. 6275, Millimeter and Submillimeter Detectors Instrumentation for Astronomy III. SPIE, Bellingham, 62751E
Holland S. T. et al., 2010, ApJ, 717, 223
Hughes D. H. et al., 1998, Nat, 394, 241
Hunt L., Palazzi E., Rossi A., Savaglio S., Cresci G., Klose S., Michałowski M., Pian E., 2011, ApJ, 736, L36
Jakobsson P., Hjorth J., Fynbo J. P. U., Watson D., Pedersen K., Björnsson G., Gorosabel J., 2004, ApJ, 617, L21
Jakobsson P. et al., 2006, A&A, 447, 897
Jaunsen A. O. et al., 2008, ApJ, 681, 453
Jenness T., Berry D., Chapin E., Economou F., Gibb A., Scott D., 2011, in Evans I. N., Accomazzi A., Mink D. J., Rots A. H., eds, ASP Conf. Ser. Vol. 442, Astronomical Data Analysis Software and Systems XX. Astron. Soc. Pac., San Francisco, p. 281
Kawai N. et al., 2006, Nat, 440, 184
Kennicutt R. C., Jr, 1998, ARA&A, 36, 189
Kistler M. D., Yüksel H., Beacom J. F., Hopkins A. M., Wyithe J. S. B., 2009, ApJ, 705, L104
Kuepcue Yoldas A., Yoldas A., Greiner J., Kruehler T., Klose S., Szokoly G., 2008, GRB Coordinates Network, 7279, 1
Küpcü Yoldaş A., Greiner J., Klose S., Krühler T., Savaglio S., 2010, A&A, 515, 2
Le Floc'h E. et al., 2003, A&A, 400, 499
Le Floc'h E., Charmandaris V., Forrest W. J., Mirabel I. F., Armus L., Devost D., 2006, ApJ, 642, 636
Levan A. et al., 2006a, ApJ, 647, 471
Levan A. J., Davies M. B., King A. R., 2006b, MNRAS, 372, 1351
Levan A. J. et al., 2007, MNRAS, 378, 1439
Levesque E. M., Kewley L. J., Graham J. F., Fruchter A. S., 2010a, ApJ, 712, L26
Levesque E. M., Kewley L. J., Berger E., Jabran Zahid H., 2010b, ArXiv e-prints
Melandri A. et al., 2008, ApJ, 686, 1209
Michałowski M. J., Hjorth J., Castro Cerón J. M., Watson D., 2008, ApJ, 672, 817
Michałowski M., Hjorth J., Watson D., 2010a, A&A, 514, A67
Michałowski M. J., Watson D., Hjorth J., 2010b, ApJ, 712, 942
Modjaz M. et al., 2008, AJ, 135, 1136
Nousek J. A. et al., 2006, ApJ, 642, 389
Overzier R. A. et al., 2011, ApJ, 726, L7
Patel M., Warren S. J., Mortlock D. J., Fynbo J. P. U., 2010, A&A, 512, L3
Pérez-Ramírez D. et al., 2010, A&A, 510, A105
Perley D. A. et al., 2009, AJ, 138, 1690
Perley D. A. et al., 2011, AJ, 141, 36
Prevot M. L., Lequeux J., Prevot L., Maurice E., Rocca-Volmerange B., 1984, A&A, 132, 389
Price P. A., Schmidt B. P., 2004, in Fenimore E., Galassi M., eds, AIP Conf. Ser. Vol. 727, Gamma-Ray Bursts: 30 Years of Discovery. Am. Inst. Phys., New York, p. 503
Racusin J. L., 2008, GRB Coordinates Network, 7266, 1
Rol E., Wijers R. A. M. J., Kouveliotou C., Kaper L., Kaneko Y., 2005, ApJ, 624, 868
Rol E. et al., 2007, ApJ, 669, 1098
Salvaterra R. et al., 2009, Nat, 461, 1258
Savaglio S., Glazebrook K., Le Borgne D., 2009, ApJ, 691, 182
Schady P. et al., 2007, MNRAS, 377, 273
Schady P. et al., 2010, MNRAS, 401, 2773
Seaton M. J., 1979, MNRAS, 187, 73p
Siebenmorgen R., Krügel E., 2007, A&A, 461, 445
Smail I., Chapman S. C., Blain A. W., Ivison R. J., 2004, ApJ, 616, 71
Smith I. A. et al., 2005, A&A, 439, 987
Stamatikos M. et al., 2008, GRB Coordinates Network, 7272, 1
Stanek K. Z. et al., 2003, ApJ, 591, L17
Svensson K. M., Levan A. J., Tanvir N. R., Fruchter A. S., Strolger L., 2010, MNRAS, 405, 57
Swinbank A. M., Smail I., Chapman S. C., Blain A. W., Ivison R. J., Keel W. C., 2004, ApJ, 617, 64
Tanvir N. R. et al., 2004, MNRAS, 352, 1073
Tanvir N. R. et al., 2008, MNRAS, 388, 1743
Tanvir N. R. et al., 2009, Nat, 461, 1254
van der Horst A. J., Kouveliotou C., Gehrels N., Rol E., Wijers R. A. M. J., Cannizzo J. K., Racusin J., Burrows D. N., 2009, ApJ, 699, 1087
Watson D., Hjorth J., Jakobsson P., Pedersen K., Patel S., Kouveliotou C., 2004, A&A, 425, L33
Wolf C., Podsiadlowski P., 2007, MNRAS, 375, 1049
Yüksel H., Kistler M. D., Beacom J. F., Hopkins A. M., 2008, ApJ, 683, L5

This paper has been typeset from a TEX/LATEX file prepared by the author.